Bioprocess Biosyst Eng (2015) 38:1325–1333
DOI 10.1007/s00449-015-1373-z

ORIGINAL PAPER

Biological capacitance studies of anodes in microbial fuel cells using electrochemical impedance spectroscopy

Zhihao Lu · Peter Girguis · Peng Liang · Haifeng Shi · Guangtuan Huang · Lankun Cai · Lehua Zhang

Received: 14 January 2015 / Accepted: 29 January 2015 / Published online: 6 February 2015

Abstract It is known that cell potential increases while anode resistance decreases during the start-up of microbial fuel cells (MFCs). Biological capacitance, defined as the apparent capacitance attributed to biological activity including biofilm production, plays a role in this phenomenon. In this research, electrochemical impedance spectroscopy was employed to study anode capacitance and resistance during the start-up period of MFCs so that the role of biological capacitance was revealed in electricity generation by MFCs. It was observed that the anode capacitance ranged from 3.29 to 120 mF which increased by 16.8 % to 18–20 times over 10–12 days. Notably, lowering the temperature and arresting biological activity via fixation by 4 % para formaldehyde resulted in the decrease of biological capacitance by 16.9 and 62.6 %, indicating a negative correlation between anode capacitance and anode resistance of MFCs. Thus, biological capacitance of anode should play an important role in power generation by MFCs. We suggest that MFCs are not only biological reactors and/or electrochemical cells, but also biological capacitors, extending the vision on mechanism exploration of electron transfer, reactor structure design and electrode materials development of MFCs.

Keywords Biological capacitance · Electrochemical impedance spectroscopy · Equivalent electrical circuit · Microbial fuel cell · Polarization resistance

Z. Lu · H. Shi · G. Huang · L. Cai · L. Zhang
State Environmental Protection Key Laboratory of Environmental Assessment and Control on Chemical Process, School of Resources and Environmental Engineering, East China University of Science and Technology, 130 Meilong Road, Shanghai 200237, China

P. Girguis · L. Zhang (✉)
Department of Organismic and Evolutionary Biology, Harvard University, 16 Divinity Avenue, Cambridge, MA 02138, USA
e-mail: lezhanghua@163.com; lezhanghua@ecust.edu.cn

P. Liang
State Key Joint Laboratory of Environment Simulation and Pollution Control, School of Environment, Tsinghua University, 30 Shuangqing Road, Beijing 100084, China

Introduction

Microbial fuel cells (MFCs) have received much attention as an alternative means of energy production from organic matter, e.g., wastewater [1, 2]. However, the high inherent voltage loss and low electrical power density obtained hinder the practical application of this technology. Many researchers have focused on minimizing voltage loss to increase electrical power density, and thus enhance the utility of MFCs [3, 4].

The concept of internal resistance has been recognized as an important indicator for voltage loss of MFCs [5, 6]. Several techniques including electrochemical impedance spectroscopy (EIS) have been applied to determine the components of internal resistance [7, 8]. EIS has been a standard tool for in situ characterization of fuel cells as well as one of the most sophisticated techniques for recognization of the internal resistance components: ohmic resistance, charge transfer resistance and diffusion resistance [9]. Recently, EIS has been applied to determine individual resistances [10–12] and the electrochemical behavior of redox mediators [13] as well as characterize anode performance in MFCs [14, 15]. It does not appear to interrupt the establishment or activity of the microbial community during the test [16], which is a notable property of EIS.

The results of EIS are analyzed combined with equivalent electrical circuit (EEC) fitting models which consist of common electric elements including resistors (R), capacitors (C), constant phase elements (CPE or Q) and inductors (W). To date, several EECs have been developed to suit a variety of MFC systems [17–21]. A simulation of EEC R(QR)(QR) was reported to determine the internal resistance in upflow MFCs [9, 16, 22, 23]. You et al. [24] reported a simulation of EEC R(QR)(CR) to determine the internal resistance of MFCs. The components of internal resistance of MFCs have been the focus of the aforementioned studies in recent years [22–25], while the understanding on capacitance of MFCs remains limited, particularly on that of the system as well as the bacteria.

Biological capacitance of biofilms has been measured to monitor bacterial adhesion and biofilm maturation during biofouling and biocorrosion in industrial water systems by EIS [26]. For MFCs, it is found that operation mode (charging and discharging) can affect the temporal patterns of current output [22, 27]. Uría et al. [27] proved that MFCs have the ability to store charge during open circuit situations in discontinuous operation mode. Liang et al. [22] developed an MFC system that an external capacitor was used to collect power from the system, and then the charged external capacitor discharged electrons to the system itself, switching into microbial electrolysis cell (MEC) mode. This alternate charging and discharging mode improved 22–32 % higher average current production of the system, compared with the control MFC [22]. And the charging and discharging behavior is associated with the biological capacitance of biofilm in the anode of MFCs, indicating that the biological capacitance of biofilm in the anode plays an important role in the improvement of power generation of MFCs in discontinuous operation mode. However, neither the biological capacitance of biofilms in the anode was measured, nor the relationship between biological capacitance and power output of MFCs was discussed.

Manohar and Mansfeld [5] reported that the capacitance value of the MFC inoculated with *Shewanella oneidensis* MR-1 in anolyte was significantly higher than that of the MFC without inoculation. To our knowledge, it is first reported about the increase of capacitance after inoculation in MFCs; however, the increasing capacitance of the inoculated MFCs was not discussed in sufficient detail [5]. Ha et al. [28] determined the charge transfer resistance and capacitance of a flat-plate type MFC with acetate as electron donor. A better comprehension of capacitance would be helpful to minimize the internal resistance and improve electrical power density of MFCs. In this study, the variation of biofilm capacitance in the anode was examined during the start-up period of three types of MFCs by means of EIS. And the effect of biological activity on the biological capacitance was investigated through lowering the temperature and arresting biological activity via fixation by 4 % para formaldehyde. Moreover, a modified equation of biological capacitance in MFCs was proposed to discuss how biological capacitance influences anode resistance and power generation in detail.

Materials and methods

MFC reactors

Three experiments were designed to measure the variation of capacitance during the start-up period of MFCs that employed with different types of electrodes for ubiquity. The schematic configurations of the lab-scale reactors constructed for these three experiments are illustrated in Fig. 1. MFC-1, MFC-2 and MFC-3 were used in Exp. 1, Exp. 2 and Exp. 3, respectively. The electrodes of MFC-1, MFC-2 and MFC-3 were graphite rods (3.0 mm diameter; Xinka Carbon Technology, Shanghai, China), graphite felts (4 cm × 3 cm × 3 mm; Xinka Carbon Technology, Shanghai, China) and graphite rods (3.0 mm diameter) with granular activated carbon sized at 3 ∼ 4 mm (60.0 ± 0.5 g; Xinka Carbon Technology, Shanghai, China) filled in compartments, respectively.

For MFC-1 and MFC-2, the volume of each compartment was 150 mL. Graphite rod or felt electrodes in both the compartments and an external resistor of 750 Ω were connected with titanium wire that formed external circuit. Cell voltages, anode and cathode potentials were recorded using a data acquisition system (DI-730, Dataq Instruments, Akron, OH) that automatically sampled every 5 min.

For MFC-3, the volume of each compartment was 112 mL The graphite rods (Xinka Carbon Technology, Shanghai, China) in both compartments and an external resistor of 100 Ω were connected by copper wire that formed the external circuit. Cell voltages and anode potentials were recorded using a data acquisition system (RBH8223h, Ruibohua Control Technology, Beijing, China) that sampled automatically every 5 min.

For all these double-chamber MFCs, the anodic and cathodic compartments were separated by a proton exchange membrane (Nafion TM117, DuPont, Wilmington, DE). The reference electrode was a saturated KCl Ag/AgCl reference (Microelectrodes, Bedford, NH). Potential difference between anode/cathode and reference electrode was measured as anode/cathode potential.

Inoculation and operation

The anolyte of MFCs consisted of (per liter): sodium acetate 1.0 g, phosphate buffered saline (PBS) 50 mM,

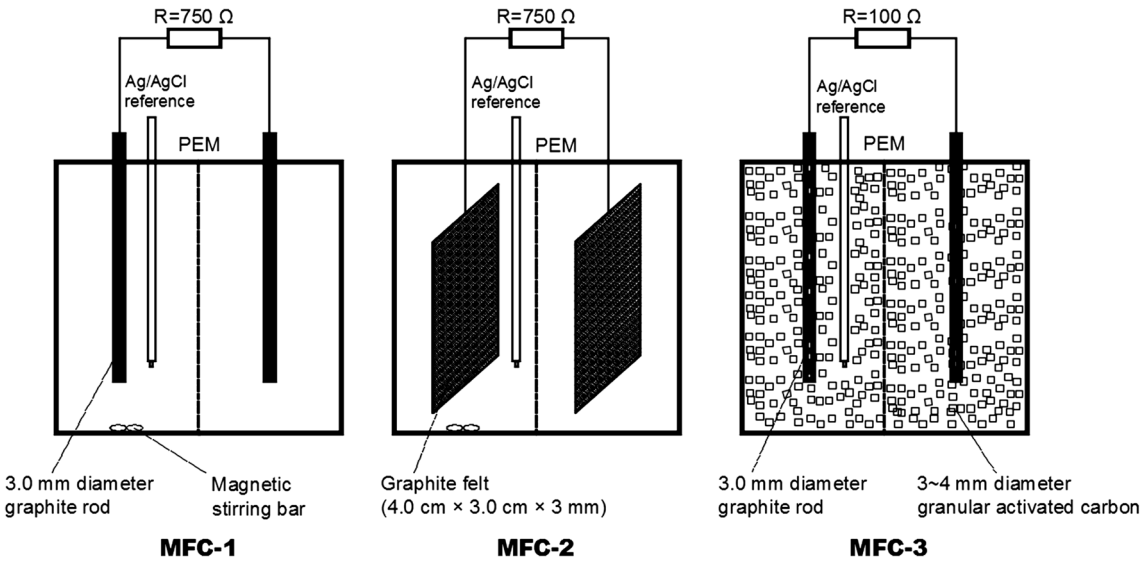

Fig. 1 Schematic configurations of lab-scale MFCs to investigate capacitance variation during the start-up period

ammonium chloride 0.5 g, magnesium sulfate 0.1 g, calcium chloride dihydrate 0.1 g, potassium chloride 0.1 g, sodium bicarbonate 1.0 g, trace element solution 1 mL [29]. Oxygen was removed from the anode solution prior to inoculation by boiling for 5 min and then sparging nitrogen gas for 30 min. Potassium hexacyanoferrate (100 mM) was provided as the electron acceptor in catholyte prepared following the literature [30].

MFC-1 and MFC-2 were inoculated with anaerobic sludge from an anaerobic biological reactor for wastewater treatment (Deer Island Wastewater Treatment Plant, Boston, MA). The MFCs were operated in fed-batch mode at 25 ± 2 °C, and both anolyte and catholyte were daily replaced for 75 mL to ensure available carbon and stable pH. The voltage output reached the maximum after 9 days operation, following the stable operation of the MFCs for another 2 days. To investigate the effect of biological activity on biological capacitance, MFC-2 was operated and the EIS tests were conducted at 0 ± 0.5 °C after the start-up period in Exp. 2. To distinguish the biological capacitance from the abiotic capacitance, at the end of Exp. 2, the graphite felt anode in MFC-2 was taken out and immersed in a 4 % para formaldehyde solution in PBS for 12 h at 4 ± 0.5 °C, then washed 3 times by PBS, and finally put back into MFC-2 for the EIS tests.

MFC-3 was inoculated with mixed cultures from the anode of a running MFC. The anolyte and catholyte flowed from the bottom of the compartments to the top through a peristaltic pump (BTl00-1L, Longer Precision Pump, Baoding, China) at a flow rate of 5 mL min^{-1}. The catholyte was continuously aerated by an air pump (RS-8801, Wanjing Pump Valve, Shanghai, China). MFC-3 was operated in continuous mode at 25 ± 2 °C. The voltage output reached the maximum after 9-day operation, following the stable operation of the MFCs for another 4 days.

EIS tests

EIS tests were conducted every 24 h, at open circuit voltages (OCVs) of MFCs against a saturated KCl Ag/AgCl reference electrode placed in close proximity to the anode [9, 16]. During each EIS test, OCVs of the MFC was confirmed as being steady. A two-electrode configuration was used that took the anode as working electrode and the cathode as the reference as well as counter electrode at 25 ± 2 °C [9, 16]. An alternating current signal with an amplitude of 10 mV and a frequency range of 10 kHz–10 mHz was applied, so as to minimize the disturbance on systematic stability and prevent biofilm detachment. EIS tests were conducted using a potentiostat (Reference 600, Gamry Instruments, Warminster, PA) in Exp. 1 and Exp. 2 and a VersaSTAT FRA analyzer (PARSTAT 2273, Princeton Applied Research, Oak Ridge, TN) in Exp. 3.

EIS data analysis

The resistance and capacitance were obtained by EECs fitting analysis of the resulting data using Gamry Echem Analyst Software (Version 6.03) in Exp. 1 and Exp. 2, and using ZSimpWin 3.1 software integrated with VersaSTAT instrument in Exp. 3.

EECs are consisted of common electric elements. The internal resistance in MFCs has been described by many researchers using EIS [10–16, 22, 23]. In this study,

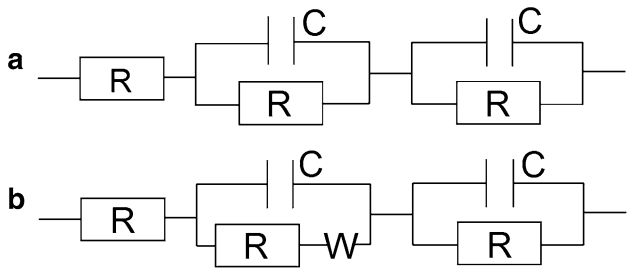

Fig. 2 EEC models used to fit EIS data during the start-up period of MFC-1 (**a**), MFC-2 (**a**) and MFC-3 (**b**). Electric elements include *R* resistors, *C* capacitors and *W* inductors

capacitance data were obtained by the EECs fitted with the EIS data of MFCs. Both capacitors and constant phase elements (CPE or Q) could substitute the capacitance in EECs. The "correct" capacitance could be calculated corresponding to the Q° and exponent sign (*n*) value of the CPE in some cases. However, the calculation precession is complicated and the "correct" capacitance is unreliable because of the inhomogeneous conditions (e.g., electrode roughness, coating and distribution of reaction rate). To simplify the EEC fitting models, the capacitor (C) was selected to substitute the capacitance in the EECs in this study. In Exp. 1 and Exp. 2, an EEC $R_o(R_aC_a)(R_cC_c)$ (Fig. 2) was used to analyze the resulting data, which consists of the elements: R_o ohm resistance, R_a anode resistance, R_c cathode resistance, C_a anode capacitance and C_c cathode capacitance. In Exp. 3, an EEC $R_o[(R_aW_a)C_a](R_cC_c)$ (Fig. 2) was used with the elements above and W_a, the diffusion resistance in anode. Warburg element (*W*) in parallel to R_a represents the simple diffusion in anode of MFC-3, which is a fixed-bed reactor.

Results

Anode potentials and cell voltages

Figure 3 showed the cell voltages and the electrode potentials in the start-up period of MFC-1, MFC-2 and MFC-3. For the first 2 days, cell voltages of MFC-1, MFC-2 and MFC-3 stayed less than 50 mV. After day 2, cell voltages began to increase while anode potentials began to decrease and cathode potentials were stable around 0.30–0.35 V. For MFC-1, the cell voltages ranged between 0.15 and 0.20 V with an external resistance of 750 Ω, while its anode potential was around 0.10 V when the MFC-1 run stably from day 10 to day 11. For MFC-2, cell voltages ranged between 0.60 and 0.70 V with an external resistance of 750 Ω, while its anode potential was around −0.40 V when MFC-2 ran stably from day 9 to day 11. For

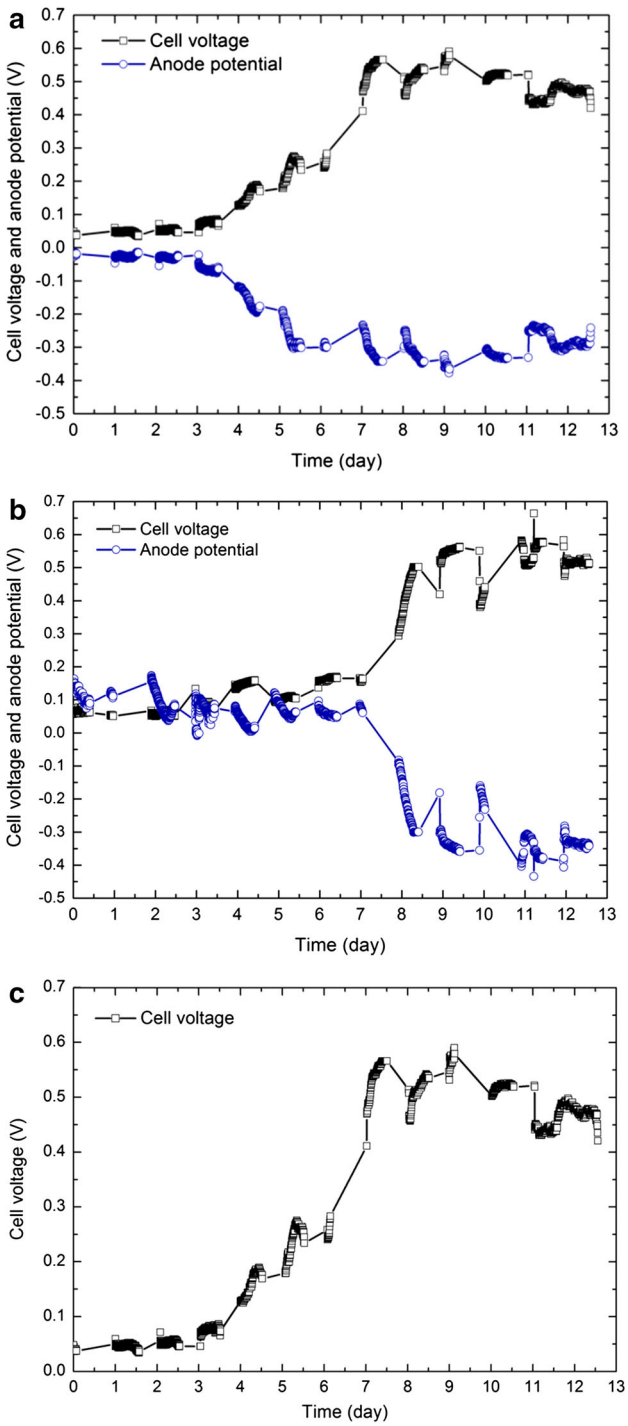

Fig. 3 Cell voltages and anode potentials (vs. a saturated KCl Ag/AgCl electrode) during start-up period of MFC-1 (**a**), MFC-2 (**b**) and MFC-3 (**c**). The external resistance of MFC-1 (**a**), MFC-2 (**b**) and MFC-3 (**c**) was 750, 750 and 100 Ω, respectively

MFC-3, cell voltages ranged between 0.47 and 0.53 V with an external resistance of 100 Ω, while anode potentials ranged between −0.27 and −0.32 V when MFC-3 ran stably from day 8 to day 12.

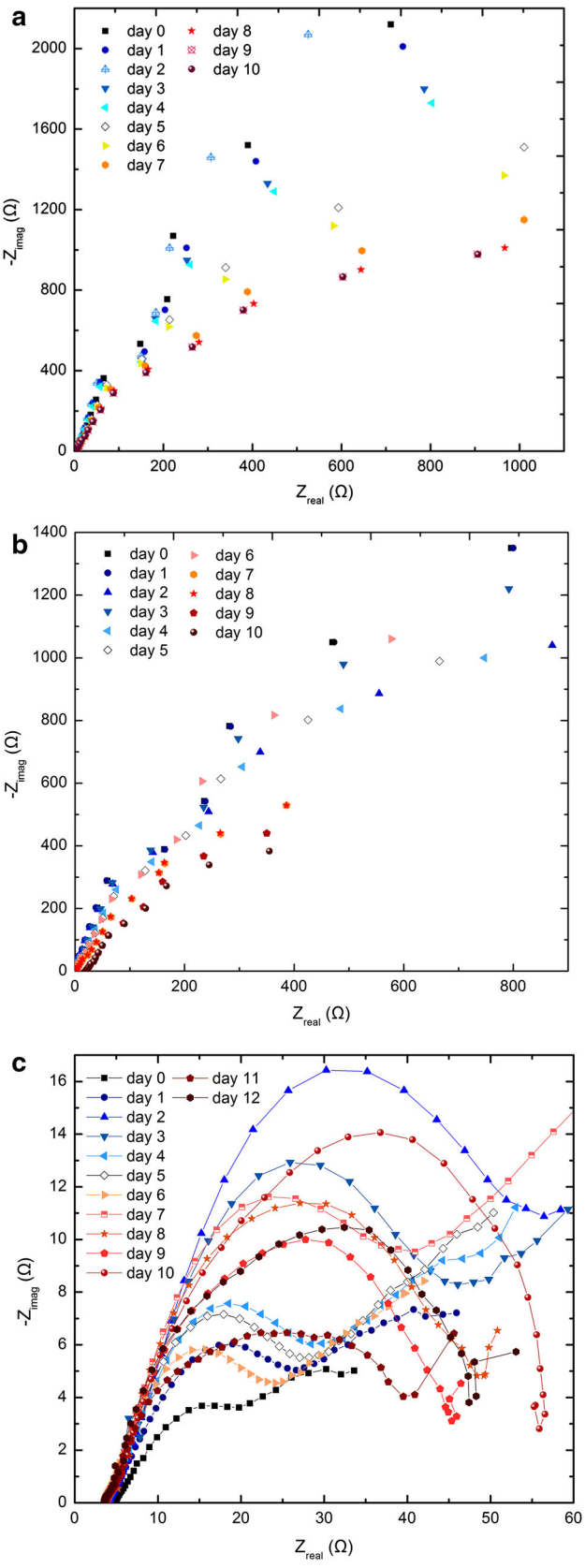

Fig. 4 Nyquist plots of EIS tests during start-up period of MFC-1 (**a**), MFC-2 (**b**) and MFC-3 (**c**). During each EIS tests, an alternating current signal with an amplitude of 10 mV and a frequency range of 10–10 mHz was applied

Nyquist plots, anode capacitance and resistance

The Nyquist plots of EIS tests for MFC-1 during 11 days with the graphite rod anode are shown in Fig. 4a, and the anode capacitance and resistance of MFC-1 are shown in Fig. 5a by fitting the impedance data to EEC $R_o(R_aC_a)(R_cC_c)$ (Fig. 2a). The anode capacitance of MFC-1 was 2.82 mF and the anode resistance was 5,084 Ω at day 1. Then, the anode capacitance increased while the anode resistance decreased during the start-up period of MFC-1. At day 11, the anode capacitance of MFC-1 was about 3.29 mF which is 16.8 % higher than that at day 1, and the anode resistance was around 1,600–1,700 Ω.

The Nyquist plots of EIS tests for MFC-2 with the graphite felt anode are shown in Fig. 4b, and the anode capacitance and resistance are shown in Fig. 5b by fitting the impedance data to EEC $R_o(R_aC_a)(R_cC_c)$ (Fig. 2a). The anode capacitance of MFC-2 during day 1–2 ranged between 3.25 and 3.29 mF, and the anode resistance ranged between 2,276 and 2,293 Ω. Then the anode capacitance increased, while the anode resistance decreased during the start-up period of MFC-2. At day 11, the anode capacitance of MFC-2 was about 7.14 mF which is 117.2 % higher than that at day 1–2, and the anode resistance was around 1,000 Ω.

The Nyquist plots of EIS tests for MFC-3 are shown in Fig. 4c, and the anode capacitance and resistance are shown in Fig. 5c by fitting the impedance data to EEC $R_o[(R_aW_a)C_a](R_cC_c)$ (Fig. 2b). The anode capacitance of MFC-3 increased from day 1 to day 6 during the start-up period, while the anode resistance decreased. From day 8 to day 12, both the anode resistance and the anode capacitance were stable when MFC-3 ran stably. The anode capacitance of 90–120 mF during day 8–12 were around 18–20 times higher than that of 3.0–6.0 mF during day 1–2. In contrast, the anode resistance of 30–35 Ω during day 1–2 was about 15–20 times higher than that of 1.5–3.0 Ω during day 8–12.

Effect of temperature on biological capacitance

The Nyquist plots, anode capacitance and resistance of MFC-2 obtained by EIS at 0 ± 0.5 and 25 ± 2 °C are shown in Fig. 6. The anode capacitance of MFC-2 was 8.59 ± 1.27 mF at 25 ± 2 °C, while decreased to 7.14 ± 0.37 mF at 0 ± 0.5 °C that dropped by 16.9 %. The anode resistance of MFC-2 was 818 ± 173 Ω at

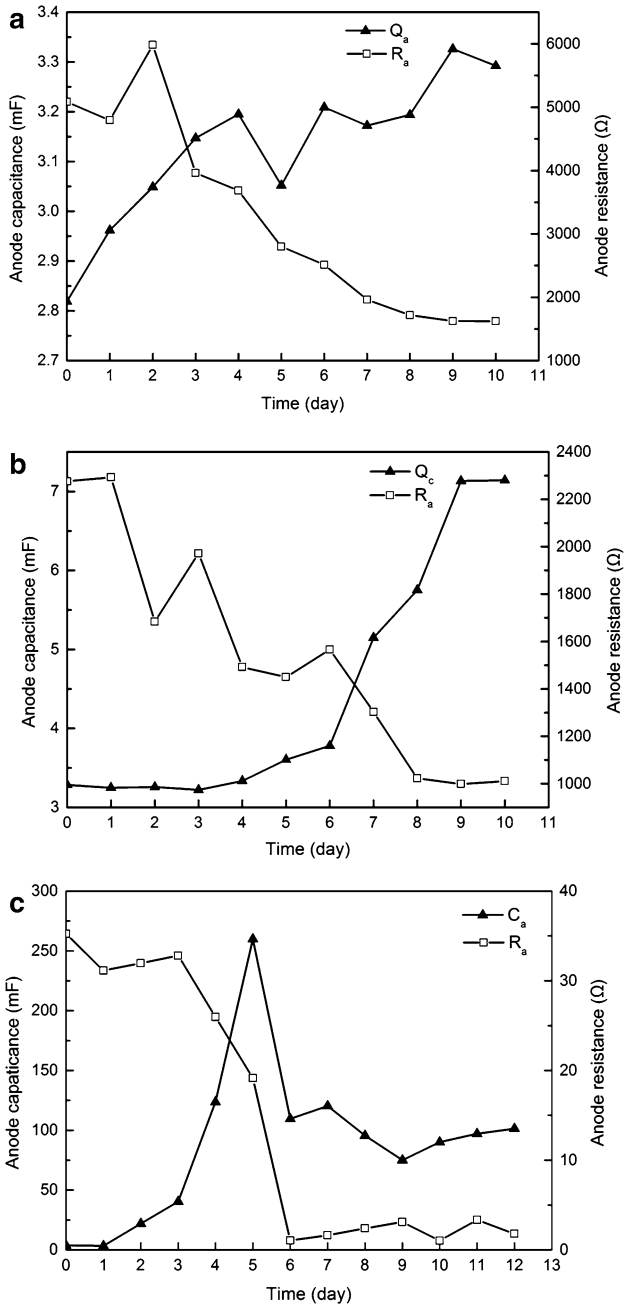

Fig. 5 Anode capacitance and resistance obtained by EIS during the start-up period of MFC-1 (**a**), MFC-2 (**b**) and MFC-3 (**c**). EEC $R_o(R_aC_a)(R_cC_c)$ was used to analyze the resulting data of MFC-1 in Exp. 1 and MFC-2 in Exp. 2; EEC $R_o[(R_aW_a)C_a](R_cC_c)$ was used to analyze the resulting data of MFC-3 in Exp. 3

25 ± 2 °C, while rose to 1,573 ± 110 Ω at 0 ± 0.5 °C, increased by 92.3 %.

Biological and abiotic capacitance

As shown in Fig. 6, the Nyquist plots, anode capacitance and resistance of MFC-1 and MFC-2 before and after cell

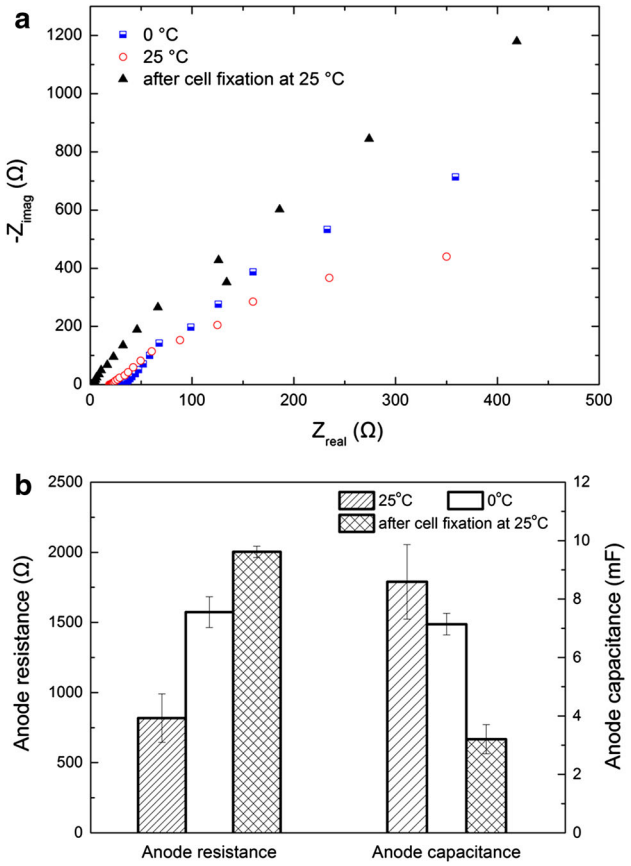

Fig. 6 Nyquist plots (**a**), anode capacitance and resistance (**b**) obtained by EIS during the start-up period of MFC-2 at 0 ± 0.5 and 25 ± 2 °C before and after cell fixation in the 4 % para formaldehyde solution for 12 h at 4 ± 0.5 °C

fixation were obtained by EIS. After cell fixation, the anode capacitance of MFC-2 was 3.20 ± 0.50 mF, decreased by 62.6 % compared with that before cell fixation (8.59 ± 1.27 mF). Biological capacitance is defined as the increasing capacitance of anode because of the vital movement of anodic electricigens. It means that the biological capacitance of anode in MFC-2 is about 5.39 mF. While the anode resistance of MFC-2 was 2,003 ± 40 Ω after cell fixation, much higher than that before cell fixation (818 ± 173 Ω).

Discussion

Membrane capacitance of electricigen cells

Membrane capacitance has been found for cell suspensions, such as muscle cells and nerve cells [31, 32]. The membrane of these cells is composed of a lipid bilayer that acts as a capacitor. Membrane capacitance plays an important functional role in synaptic integration and signal

propagation that determines the amplitude of the postsynaptic potential at the site of a fast synaptic input [31, 32]. For electricigen cells, the cell membrane is of a phospholipid bilayer structure that acts as a capacitor. Besides, electron shuttles (or redox mediators) [33], *c*-type cytochromes [34] and nanowires [35] in/on cell membrane endogenously produced by electricigen cells work as electrochemically active sites [33–36]. Therefore, the biological capacitance of MFC anode increases with the anodic electricigen amount as well as the electrochemical activity. Further research is interesting to explore the differences of biological capacitance among biological tissue systems, electricigens and non-electricigens.

Influencing factors of biological capacitance

For a panel capacitor, the calculation equation for capacitance is:

$$C = \frac{\varepsilon S}{4\pi k d}, \tag{1}$$

where C is the capacitance, ε is the dielectric constant, S is the contact area, k is the electrostatic constant (9×10^9 $\mathrm{Nm^2\ C^{-2}}$) and d is the distance between the plates. During the start-up period of MFCs, the main bioprocesses include both the multiplication and the electrochemical activity increase of anode electricigens (shown in Fig. 7). The electricigens attached to the anode grew in form of biological membrane. The effective surface area and anode capacitance of MFCs increased with the amount of anode electricigens according to Eq. (1). Additionally, the higher electrochemical activity of the anode electricigens, the more electron shuttles or redox mediators (e.g., *c*-type cytochromes or nanowires in cell membranes) working as the electrochemical activity, and then the greater effective "surface area" of the pseudocapacitor in the EEC. Therefore, the capacitance of MFCs increased with the increasing amount of anode electricigens as well as electron shuttles according to Eq. (1). Thus, the equation calculating the anode capacitance of MFCs could be modified as:

$$C = K\varepsilon \times \frac{NAS}{4\pi k d}, \tag{2}$$

where C is the anode capacitance of MFCs, K is the coefficient, N is the amount of anode electricigens and A is the amount of electron shuttles, *c*-type cytochromes and nanowires in/on the cell membrane per electrigen cell.

The anode capacitance of MFC-1, MFC-2 and MFC-3 were 3.29, 7.14 and 90–120 mF, and they increased by 16.8, 117.2 % and 18–20 times than those at day 1, respectively. According to Eq. (1), we believe that the difference of MFC-1, MFC-2 and MFC-3 construction (Fig. 1) resulted in the difference of increasing anode capacitance. The amount of the anode biomass and electricigens in MFC-3 was more than that of MFC-2 while the amount of the anode biomass and electricigens of MFC-2 was more than that of MFC-1. Therefore, the increasing anode capacitance of MFC-3 was more than that of MFC-2 and the increasing anode capacitance of MFC-2 was more than that of MFC-1.

Anode capacitance and resistance

The MFC has a characteristic amount of capacitance per unit of power production capability. If there is more electricigen biomass in contact with the electrode, then there will be more power production and more capacitance. Polarization resistance is simply the inverse of the power production capability. The more the power produced at a specific voltage, in accordance with Ohm's Law, the lower the "resistance" of the power generator. The concept of "polarization resistance" in a fuel cell is a metaphor. There is no resistor, but merely effective limitations to power production capacity. Capacitance is the buffering, or power backup, capability of the power plant, which can interpret the previous result that bacterial capacitance is an effective compensation to eliminate power overshoot in MFCs [37]. There is a characteristic amount of backup capability per unit of power production. Therefore, it is in direct proportion to the amount of electricigen biomass in contact with the electrode.

During the start-up period of MFC-1, MFC-2 and MFC-3, the anode capacitance increased while the anode resistance decreased. The anode resistance of MFC-1, MFC-2 and MFC-3 decreased by 67.5, 56.4 and 91.6 %, respectively, compared with those at day 1. It is well known that the anode resistance is inversely correlated with the area of anode and the amount as well as the activity of anode electricigens [5]. The anode polarization resistance could be described as:

$$R_a = K' \times \frac{1}{NAS} \tag{3}$$

$$CR_a = KK'\varepsilon \times \frac{1}{4\pi k d}, \tag{4}$$

where K' and K are the coefficients. When the setting value of the dielectric constant (ε) and the distance between anode and cathode (d) were given in this research, the value $\left(KK'\varepsilon \times \frac{1}{4\pi k d}\right)$ of C multiplied by R_a is a setting value, meaning that the anode capacitance of MFCs is in inverse correlation with the anode polarization resistance. The Pearson product-moment correlation coefficient between C and R ranged between -0.77 and -0.82 (Fig. 5), suggesting a large strength of association between C and R.

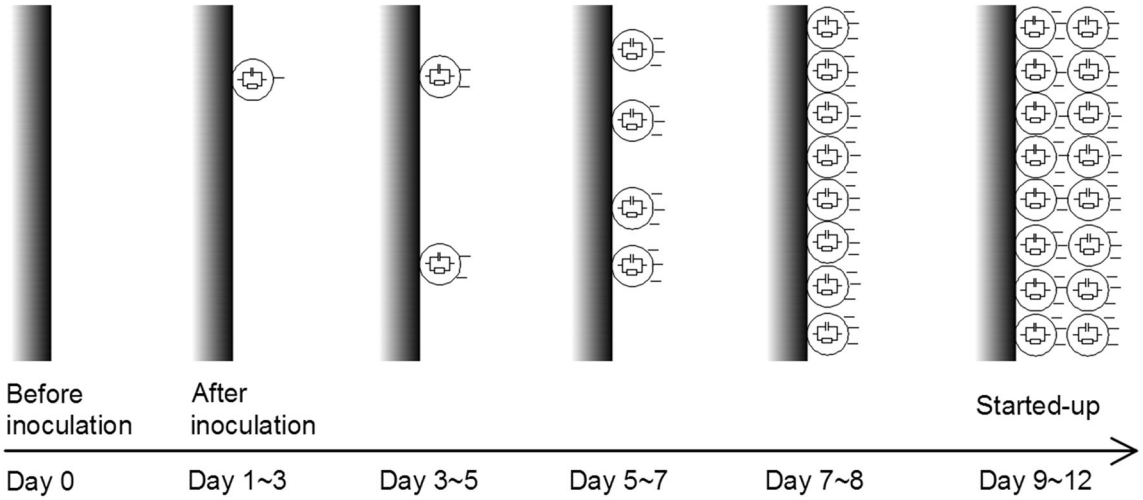

Fig. 7 Multiplication and increasing electrochemical activity of electricigens on anode surface during start-up period of MFCs (is anode, is electricigen and — is the electron on cell surface of electricigens)

Implication of power generation by MFCs

MFC is a biofuel cell in which electrochemical active microorganisms (EAMs) function as catalysts to convert chemical energy into electrical energy. To date, most researchers have investigated MFCs as biological reactors and/or electrochemical cells based on their purposes of study. Anode capacitance of MFCs increases with increasing power production and decreasing anode resistance during start-up period of MFCs. The results reveal that MFCs are not only biological reactors and/or electrochemical cells, but also capacitors, which opening up a vision of exploring the electron transfer mechanisms, designing reactor structure and developing electrode materials, e.g., increasing the biological capacitance of anode could result in an increasing power density. The Pearson product-moment correlation coefficient between C and P ranged between 0.73 and 0.97 (Figs. 3, 5), suggests a large strength of association between C and P. Additionally, the volume of anode compartment should be hundreds or thousands cubic meters if the MFCs would be designed to treat wastewater for practical applications in the future. In this case, the biomass and its biological capacitance should play an important role in power generation by MFCs because MFCs are of supercapacitors likewise.

Conclusions

In this study, the capacitance variation of MFCs was investigated, as well as the relation with working voltages, OCVs, internal resistance of MFCs, etc. The results showed that MFCs' capacitance gradually increased after a decrease during the set-up period. Anode capacitance change is not consistent completely with the anode potential and cell voltage output changes. The capacitance of MFCs was positively correlated with the anode potential and cell voltage output during day 3–6. The capacitance change was consistent with the open circuit voltage change that gradually increased during day 3–11, while remained stable after 11 days. The capacitance of MFCs is negatively correlated with the internal resistance of MFCs that the total resistance increased while the capacitance decreased during day 1–2 after inoculation, and the total resistance decreased while the capacitance increased during day 3–11. It is indicated that MFCs are not only biological reactors and/or electrochemical cells, but also biological capacitors.

Acknowledgments This research is supported by the National Natural Science Foundation of China (NSFC) (20906026), Shanghai Pujiang Program (09PJ1402900), the Fundamental Research Funds for the Central Universities (WB0914036) and the Scientific Research Foundation for the Returned Overseas Chinese Scholars, State Education Ministry (B200-C-0904).

References

1. Ha PT, Lee TK, Rittmann BE, Park J, Chang IS (2012) Treatment of alcohol distillery wastewater using a Bacteroidetes-dominant thermophilic microbial fuel cell. Environ Sci Technol 46(5):3022–3030
2. Werner CM, Logan BE, Saikaly PE, Amy GL (2013) Wastewater treatment, energy recovery and desalination using a forward osmosis membrane in an air-cathode microbial osmotic fuel cell. J Membrane Sci 428:116–122
3. Clauwaert P, Aelterman P, Pham TH, De Schamphelaire L, Carballa M, Rabaey K, Verstraete W (2008) Minimizing losses in

bio-electrochemical systems: the road to applications. Appl Microbiol Biot 79(6):901–913
4. Rismani-Yazdi H, Carver SM, Christy AD, Tuovinen OH (2008) Cathodic limitations in microbial fuel cells: an overview. J Power Sources 180(2):683–694
5. Manohar AK, Mansfeld F (2009) The internal resistance of a microbial fuel cell and its dependence on cell design and operating conditions. Electrochim Acta 54(6):1664–1670
6. Ha PT, Moon H, Kim BH, Ng HY, Chang IS (2010) Determination of charge transfer resistance and capacitance of microbial fuel cell through a transient response analysis of cell voltage. Biosens Bioelectron 25(7):1629–1634
7. Logan BE, Hamelers B, Rozendal R, Schröder U, Keller J, Freguia S, Aelterman P, Verstraete W, Rabaey K (2006) Microbial fuel cells: methodology and technology. Environ Sci Technol 40(17):5181–5192
8. Ciureanu M, Roberge R (2001) Electrochemical impedance study of PEM fuel cells. Experimental diagnostics and modeling of air cathodes. J Phys Chem B 105(17):3531–3539
9. He Z, Mansfeld F (2009) Exploring the use of electrochemical impedance spectroscopy (EIS) in microbial fuel cell studies. Energ Environ Sci 2(2):215–219
10. Srikanth S, Marsili E, Flickinger MC, Bond DR (2008) Electrochemical characterization of *Geobacter sulfurreducens* cells immobilized on graphite paper electrodes. Biotechnol Bioeng 99(5):1065–1073
11. Ramasamy RP, Ren Z, Mench MM, Regan JM (2008) Impact of initial biofilm growth on the anode impedance of microbial fuel cells. Biotechnol Bioeng 101(1):101–108
12. Jung S, Mench MM, Regan JM (2011) Impedance characteristics and polarization behavior of a microbial fuel cell in response to short-term changes in medium pH. Environ Sci Technol 45(20):9069–9074
13. Ramasamy RP, Gadhamshetty V, Nadeau LJ, Johnson GR (2009) Impedance spectroscopy as a tool for non-intrusive detection of extracellular mediators in microbial fuel cells. Biotechnol Bioeng 104(5):882–891
14. Yong YC, Dong XC, Chan-Park MB, Song H, Chen P (2012) Macroporous and monolithic anode based on polyaniline hybridized three-dimensional graphene for high-performance microbial fuel cells. ACS Nano 6(3):2394–2400
15. Yong YC, Yu YY, Zhang X, Song H (2014) Highly active bidirectional electron transfer by a self-assembled electroactive reduced-graphene-oxide-hybridized biofilm. Angew Chem Int Edit 53(17):4480–4483
16. He Z, Wagner N, Minteer SD, Angenent LT (2006) An upflow microbial fuel cell with an interior cathode: assessment of the internal resistance by impedance spectroscopy. Environ Sci Technol 40(17):5212–5217
17. O'Hayre R, Cha SW, Colella W, Prinz FB (2006) Fuel cell fundamentals. Wiley, New york
18. Manohar AK, Bretschger O, Nealson KH, Mansfeld F (2008) The use of electrochemical impedance spectroscopy (EIS) in the evaluation of the electrochemical properties of a microbial fuel cell. Bioelectrochemistry 72(2):149–154
19. Kim JR, Premier GC, Hawkes FR, Dinsdale RM, Guwy AJ (2009) Development of a tubular microbial fuel cell (MFC) employing a membrane electrode assembly cathode. J Power Sour 187(2):393–399
20. Min B, Cheng S, Logan BE (2005) Electricity generation using membrane and salt bridge microbial fuel cells. Water Res 39(9):1675–1686
21. Navarro A, del Rio C, Acosta JL (2009) Pore-filling electrolyte membranes based on plasma-activated microporous PE matrices and sulfonated hydrogenated styrene butadiene block copolymer (SHSBS): single cell test and impedance spectroscopy in symmetrical mode. Solid State Ionics 180(32):1505–1510
22. Liang P, Wu W, Wei J (2011) Alternate charging and discharging of capacitor to enhance the electron production of bioelectrochemical systems. Environ Sci Technol 45(15):6647–6653
23. Borole AP, Aaron D, Hamilton CY, Tsouris C (2010) Understanding long-term changes in microbial fuel cell performance using electrochemical impedance spectroscopy. Environ Sci Technol 44(7):2740–2745
24. You S, Zhao Q, Zhang J, Liu H, Jiang J, Zhao S (2008) Increased sustainable electricity generation in up-flow air-cathode microbial fuel cells. Biosens Bioelectron 23(7):1157–1160
25. Dhirde AM, Dale NV, Salehfar H, Mann MD, Han TH (2010) Equivalent electric circuit modeling and performance analysis of a PEM fuel cell stack using impedance spectroscopy. IEEE T Energy Conver 25(3):778–786
26. Kim T, Kang J, Lee JH (2011) Influence of attached bacteria and biofilm on double-layer capacitance during biofilm monitoring by electrochemical impedance spectroscopy. Water Res 45(15): 4615–4622
27. Uría N, Muñoz Berbel X, Sánchez O, Muñoz FX, Mas J (2011) Transient storage of electrical charge in biofilms of *Shewanella oneidensis* MR-1 growing in a microbial fuel cell. Environ Sci Technol 45(23):10250–10256
28. Ha PT, Moon H, Kim BH, Ng HY, Chang IS (2010) Determination of charge transfer resistance and capacitance of microbial fuel cell through a transient response analysis of cell voltage. Biosens Bioelectron 25(7):1629–1634
29. Rabaey K, Ossieur W, Verhaege M, Verstraete W (2005) Continuous microbial fuel cells convert carbohydrates to electricity. Water Sci Technol 52(1):515–523
30. Rabaey K, Van de Sompel K, Maignien L, Boon N, Aelterman P, Clauwaert P, De Schamphelaire L, Pham HT, Vermeulen J, Verhaege M, Lens P, Verstraete W (2006) Microbial fuel cells for sulfide removal. Environ Sci Technol 40(17):5218–5224
31. Gentet LJ, Stuart GJ, Clements JD (2000) Direct measurement of specific membrane capacitance in neurons. Biophys J 79(1): 314–320
32. Asami K (2002) Characterization of biological cells by dielectric spectroscopy. J Non-Crystal Solids 305(1):268–277
33. Hernandez ME, Newman DK (2001) Extracellular electron transfer. Cell Mol Life Sci 58(11):1562–1571
34. Tremblay PL, Summers ZM, Glaven RH, Nevin KP, Zengler K, Barrett CL, Qiu Y, Palsson BO, Lovley DR (2011) A *c*-type cytochrome and a transcriptional regulator responsible for enhanced extracellular electron transfer in *Geobacter sulfurreducens* revealed by adaptive evolution. Environ Microbiol 13(1):13–23
35. Strycharz-Glaven SM, Snider RM, Guiseppi-Elie A, Tender LM (2011) On the electrical conductivity of microbial nanowires and biofilms. Energ Environ Sci 4(11):4366–4379
36. Yang Y, Xu M, Guo J, Sun G (2012) Bacterial extracellular electron transfer in bioelectrochemical systems. Process Biochem 47(12):1707–1714
37. Peng X, Yu H, Yu H, Wang X (2013) Lack of anodic capacitance causes power overshoot in microbial fuel cells. Bioresource Technol 138:353–358